Development of A Compact and Low Profile Cavity Backed Slot Antenna Using Microstrip Gap Waveguide Technology

A. Moghimizadeh, Seyed Ali Razavi Parizi, M. H. Ostovarzadeh
Department of Electrical and Computer Engineering, Graduate University of Advanced Technology, Kerman, Iran
azin.moghimi@yahoo.com, s.razaviparizi@kgut.ac.ir, mh.ostovarzadeh@kgut.ac.ir
Corresponding author: s.razaviparizi@kgut.ac.ir

Abstract- Proof of concept of a cavity backed slot antenna based on inverted microstrip gap waveguide (IMGW) technology is presented. Since the antenna is operating based on the first resonating mode of the cavity, it is more compact compared to the ordinary cavity backed slot antennas in which the second cavity mode is used for radiation. Furthermore, the proposed antenna element introduces lower losses compared to a microstrip patch thanks to the surface wave suppression and lower dielectric loss of the air filled IMGW cavity. A sample antenna is designed and fabricated to operate at 9.6 GHz and quite good agreement between simulation and measurement results is observed.

Index Terms- cavity backed, compact, gap waveguide, microstrip, slot antenna

I. INTRODUCTION

Cavity backed slot antennas (CBSAs) are a class of antennas that have been used in wireless telecommunications. One-sided radiation, enhances a CBSA gain compared to the double sided radiators. More ever the surface waves are suppressed in CBSA structures which increases the antenna efficiency.

Different technologies including Conventional metallic waveguides and substrate integrated waveguide (SIW) have been used to implement CBSAs [1-3]. Metal waveguides are low loss but bulky structures which makes them inappropriate for integrated modern wireless systems. SIW structures are planar and can be easily integrated with other planar circuits but they introduce more losses compared to metal waveguides.

Gap waveguide (GW) technology has been introduced recently for implementation of microwave component devices. Principles of this new technology are discussed in [4-5]. Gap waveguide structure, unlike the microstrip structures, is electrically closed and inherently provides packaging [6]. Furthermore, in GW technology the transmission line is formed in an air gap getting rid of the

Manuscript received 18-Feb.-2019 and revised 10-Aug.-2019, *P- ISSN: 2322-4088*
Accepted on 5- Nov.-2019 *E- ISSN: 2322-3936*

dielectric loss associated with microstrip and SIW structures. In addition, there is no need to create electrical contact between GW plates which makes its fabrication process easy and straight forward. This fact gives the GW technology a great advantage in fabrication point of view especially at high frequencies compared to conventional metallic waveguides. Three different types of gap waveguides including groove gap waveguide (GGW), ridge gap waveguide (RGW) and inverted microstrip gap waveguide (IMGW) have already been studied in [5].

In this paper, a proof of concept of CBSA based on IMGW technology is presented. First an IMGW cavity is designed and investigated, then a CBSA is realized by introducing a slot which is excited by the first cavity mode TM_{010}. As the proposed antenna is operating based on the first mode of IMGW cavity, it is more compact compared to the GGW cavity backed slot antenna presented in [7] in which the slot is excited by the second mode of GGW cavity (TE_{120} mode). Furthermore, the proposed antenna element, unlike the ordinary microstrip patch antennas, is inherently packaged (thanks to the gap wave technology) and can be easily integrated with other planar IMGW circuits. The proposed antenna element benefits from lower losses and higher efficiency compared to a microstrip patch antenna, especially in array form, thanks to the surface wave suppression and introducing lower dielectric loss. As a result, at mm-wave frequencies where microstrip patch arrays are very lossy, the proposed antenna element can be considered as a good alternative solution.

A prototype of the proposed structure is designed and fabricated. Quite good agreement between simulation and measurement results confirms the validity of all simulation results.

II. IMGW CAVITY

In Fig. 1 the IMGW cavity is shown. As illustrated, a rectangular patch is printed on a substrate backed by a periodic pin surface which provides PMC boundary condition for a limited frequency range called stop band. The design guidelines for the pin surface are presented in [8-10]. There is an air gap with the thickness "*g*" between upper PEC plate and the substrate. As long as the air gap thickness is less than quarter wavelength [10], the pin surface can create a stop band for parallel plate modes suppressing the wave propagation in the air gap between upper plate and the substrate. As a result, the fields are trapped in the air gap between upper PEC plate and the metal patch forming an IMGW cavity. It is well known that the PMC boundary condition is frequency dependent which confines the IMGW cavity bandwidth. The frequency range over which the the PMC bounadry condition and consecuently IMGW cavity can be established is determined by the pin surface stop band. In [10] it has shown that the smaller air gap provides wider stop band for the pin surface leading to wider bandwidth for the structure. So, in the design process, the parameter "g" is chosen a small fraction of wavelength (smaller than $\lambda/20$) to minimize the effect of the stop band limitations on the operating bandwidth. Furethuremore, The pins height "*d*" has to be approximately equal to $\lambda/4$ however the pins period "*p*" should be smaller than $\lambda/2$ keeping a/p ratio less than one.

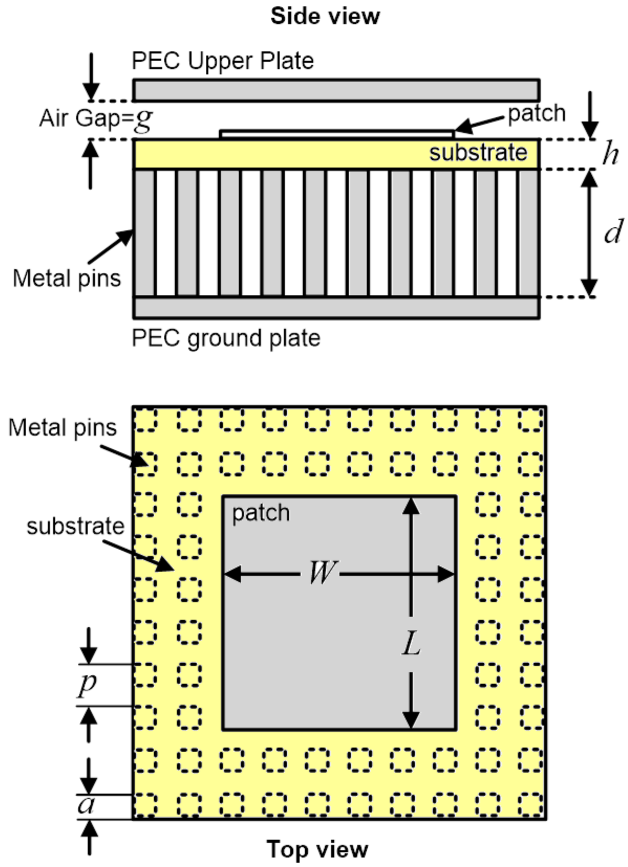

Fig. 1. Realized IMGW cavity.

The boundary conditions of this cavity are similar to the RGW cavity presented in [11]. We see that the PEC patch is caged by PMC area while a PEC plate is placed on its top with an air gap. In this case a cavity is formed in the air gap between the upper PEC wall and the patch which is called IMGW cavity. According to the boundary conditions we can consider the same approximate analytical model presented in [11], a hollow cavity with PEC broad walls and PMC side walls, which is similar to the cavity model of a microstrip patch. As a result, the resonating modes of presented IMGW cavity are the same as those supported by a microstrip patch. The cavity model of a microstrip patch is fully analyzed in [12]. So here we used the same formulas obtained in [12] for designing the cavity dimensions "*L*" and "*W*".

In our design, the pin dimensions including "*p*", "*a*", "*d*", the air gap (shown in Fig. 1) and the substrate parameters including "*h*" and "ε_r" are chosen so that a stop band is provided over 9-15GHz frequency band. The initial values for parameters "*p*", "*a*", "*d*" and "g" are chosen based on the rules mentioned before however then fine tuning is needed using a simulation model in CST. The substrate parameters "*h*" and "ε_r" are also determined with this simulation model. For this purpose, a unit cell containing a pin capped by the substrate and the air gap is simulated with CST Eigen mode solver and

TABLE I
GEOMETRICAL PARAMETERS OF THE DESIGNED IMGW CAVITY BACKED SLOT ANTENNA

parameter	Value (mm)	parameter	Value (mm)
d	6	L	10.4
h	0.8	l_s	12.8
g	1.5	w_s	1
p	5.4	w_g	0.5
a	2.3	l_g	4.6
W	15	s	2

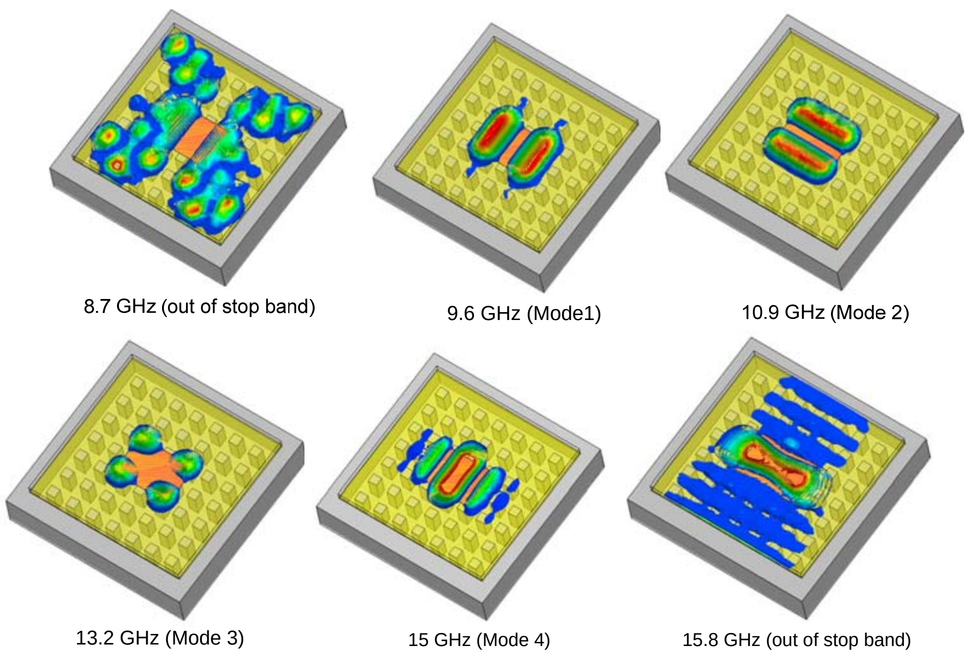

Fig. 2. Electrical field distribution inside the air gap at different frequencies in and out of pins stob band.

its dispersion diagram is extracted from which the stop band can be determined. It should be noted that in this model, the unit cell is surrounded by periodic boundaries in order to model an infinite pin surface.

Based on above descriptions, a sample rectangular shaped IMGW cavity is designed so that its first resonance occurs at 9.6 GHz. The dimensions of designed cavity are listed in Table I. In this design, Rogers Duriod 5880 with ε_r of 2.2 is used as the substrate. The designed IMGW cavity is simulated using the Eigen mode solver of HFSS software. In Fig. 2 the field distribution inside the air gap is illustrated at different frequencies in and out of pin surface stop band. As mentioned before, the IMGW cavity boundary condition is frequency dependent with the bandwidth limited by the pins stop band. This means that the IMGW cavity has limited bandwidth with few resonating modes. In Fig. 2 we see that inside the stop band (9-15GHz) an IMGW cavity is properly established with resonating modes similar to those of a rectangular shaped microstrip patch, however at the out of band frequencies the IMGW cavity is not established. The designed cavity can only support the first four resonating modes due to the bandwidth limitation, however in order to exceed the number of supported modes, the pin surface with wider stop band should be designed. In our design since the presented antenna is based on the first resonating mode TM010 wider stop band is not needed.

III. ANTENNA PRINCIPLE AND DESIGN

According to the field distribution illustrated in Fig. 2, a cavity backed slot antenna can be developed by introducing a slot to the top metal plate of the proposed IMGW cavity when operating at its first resonating mode (Mode 1 shown in Fig. 2). In Fig. 3 the slot and its location is shown. By this way the slot, according to the field distribution shown in Fig. 2, is perpendicular to the surface currents of TM_{010} mode (Mode 1) and therefore can radiate effectively. The slot length should be $\lambda/2$, where λ is the wavelength in free space, in order to achieve broadside radiation. Maximum radiation efficiency can also be achieved if the slot resonates at the resonance frequency of TM_{010} mode.

The patch is connected to a strip feed line from the side as shown in Fig. 3. By this way, according to the field distribution shown in Fig. 2, the TM_{010} mode in IMGW cavity can be excited by a TEM based IMGW feed line. The feed line geometrical parameters "*s*", "*lg*" and "*wg*" are chosen so that the proper input impedance matching is obtained. The dimensions of radiating slot and the feed line for the designed antenna can be found in Table I.

The proposed IMGW cavity backed slot antenna is working based on its first cavity mode TM_{010} for which the cavity length is quite half wavelength. As a result, the proposed antenna is more compact than its GGW counterpart presented in [7] where the second cavity mode TE_{120}, for which the cavity length is quite one wavelength, excites the radiating slot.

In compare with a simple microstrip patch antenna, the proposed antenna has the advantage of lower losses and consequently higher efficiency thanks to surface wave suppression and introducing lower dielectric loss. This superiority is more considerable in array forms. So, at mm-wave frequencies where microstrip patch arrays are very lossy, the proposed element can be considered as a good alternative solution.

III. RESULTS AND DISCUSSION

The designed antenna in previous section is simulated using HFSS. In Fig. 4(a) the current distribution on the broad wall of IMGW cavity in which the radiating slot is etched, is illustrated at 9.6 GHz. It can be clearly observed that this current distribution is accosiated with the first IMGW cavity mode TM_{010} which is perturbed by a rectangular slot. The current distribution around the slot reveals that the TM_{010} mode is effectively radiated to the outer space. This fact is also well confirmed in Fig. 4(b) in which the depicted E-field distribution across the slot shows that the slot can radiate the same as a magnetic dipole antenna, i. e. providing narrow band broadside radiation.

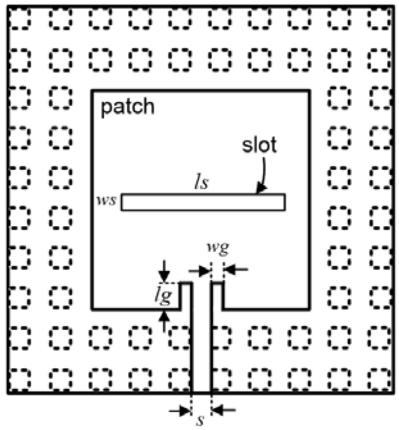

(a)

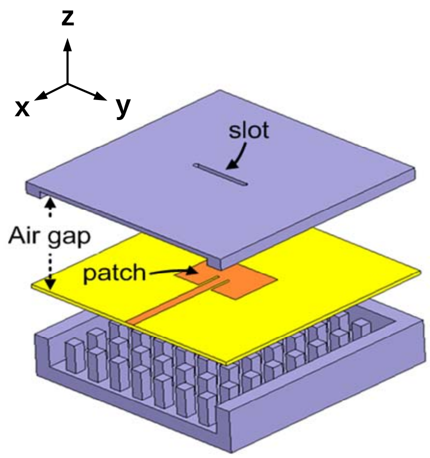

(b)

Fig. 3. Designed IMGW cavity backed slot antenna (a) Geometrical parameters of the radiating slot and feed line (b) 3D distributed view.

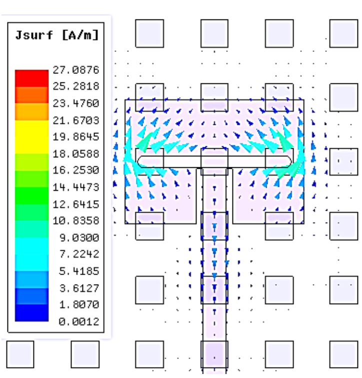

(a)

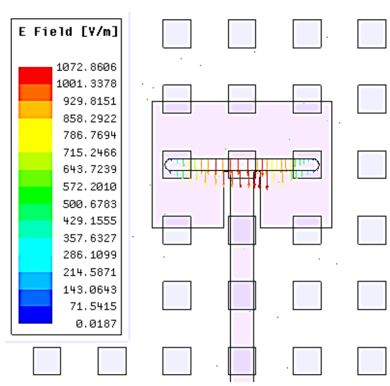

(b)

Fig. 4. The field distribution associated with the radiating mode at 9.6 GHz (a) Current distribution on the broad wall of IMGW cavity in which the slot is etched (b) E-field distribution across the slot.

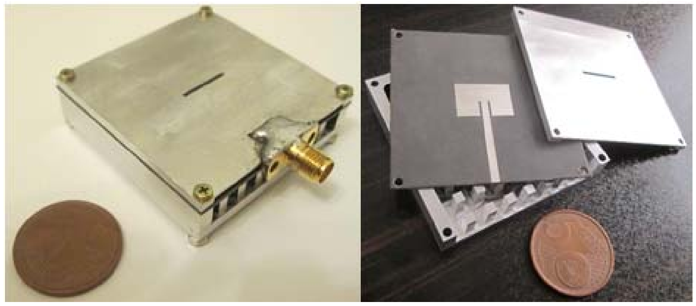

Fig. 5. Fabricated prototype.

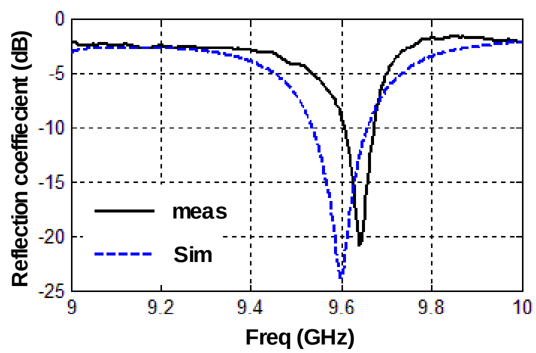

(a)

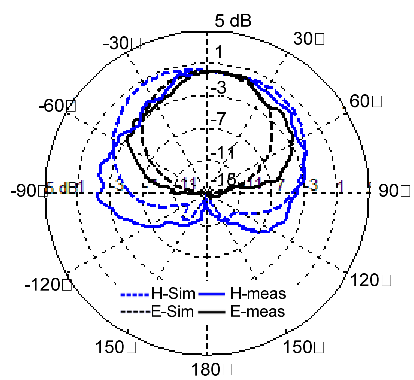

(b)

Fig. 6. Comparison between simulated and measured results (a) S_{11} (b) Radiation patterns. simulated/measured pattern in E/H-plane.

The simulated S_{11} result shown in Fig. 6(a) reveals that the designed antenna is operating at 9.6 GHz with about 1 % bandwidth ($S_{11} < -10$dB) however the measurement result shows a little bit frequency shift in operating frequency. The fair consistency between simulated and measured reflection confidents may due to the error in feed assembly. In fact, in the assembly process, the Teflon thickness of the coaxial line in which the TEM wave is propagating may not be exactly matched with the air gap thickness in IMGW line which can affect the coupling and impedance matching between coaxial line and MGW line. In Fig. 6(b), the radiation patterns in E- plane (x-z plane)

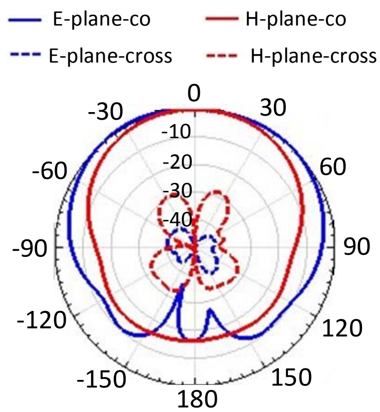

Fig. 7. Simulated cross polar radiation patterns of the designed structure in E-& H-planes (x-z & y-z planes respectively) depicted with co polar counterparts.

TABLEII

DIMENSIONS OF THE ANTENNAS PRESENTED IN [7] AND IN THIS PAPER

Antenna	Technology	Whole Dimensions
In [7]	GGW	1.56λ × 1.56λ
This paper	IMGW	1.1λ × 1.1λ

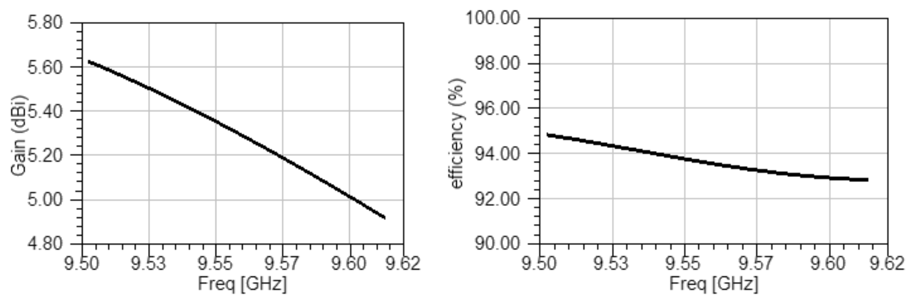

(a) (b)

Fig. 8. The (a) antenna gain variation and (b) efficiency over the operating bandwidth.

and H-plane (z-y plane) are shown at 9.6 GHz. Both simulation and measurement results show broadside radiation performance. A little discrepancy between simulated and measured radiation patterns is probably due to the parasitic radiation from SMA connector used for measurement process. In Fig. 7 the simulated cross polar radiation patterns in E-& H-planes are depicted with co-polar counterparts. The cross polar level (CPL) of below -30dB shows the proper radiation performance of the proposed structure in generation of pure linear polarization. We also measured the cross polar radiation however since the dynamic range of the anechoic chamber that we used was 20dB, no cross polar radiation was sensed in measurement process which confirms that the cross polar level is below -20dB however there is nothing to show here. Fig. 8(a) shows the antenna gain at its maximum radiation direction over the operating bandwidth. We see the maximum gain of 5.6 dBi with 0.8 dB variation. In Fig. 8(b) the designed antenna efficiency over its operating bandwidth is shown. The efficiency of more than 93% confirms the low loss nature of the proposed structure as the propagating fields are almost confined in the air gap inside the structure.

In Table II, the whole dimensions of the designed IMGW cavity backed slot antenna are compared with those of its GGW counterpart presented in [7] and we see that the proposed antenna is more compact by about 40% reduction in size.

IV. CONCLUSION

Proof of concept of a cavity backed slot antenna based on IMGW technology is presented. First, IMGW cavity was investigated and it was shown that the analytical cavity model used for a microstrip patch can also be used for this cavity. Then a cavity backed slot antenna was designed by introducing a slot to the cavity top plate so that perpendicularly cut the surface currents associated with the first cavity mode. It was also observed that using the first cavity mode for exciting the slot gives more compactness to the presented element compared to the ordinary cavity backed slot antennas in which the second resonating mode inside the cavity is used for radiation. The developed antenna performance was investigated using both simulation and measurement processes and good broadside radiation performance was observed.

REFERENCES

[1] J. Hirokawa, H. Arai, and N. Goto, "Cavity-backed wide slot antenna," *IEE Proceedings*, vol. 136, no. 1, pp. 29-33, Feb. 1989.

[2] G. Q. Luo, Z. F. Hu, L. X. Dong, and L. L. Sun, "Planar slot antenna backed by substrate integrated waveguide cavity," *IEEE Antennas and Wireless Propagation Lett.*, vol. 7, pp. 236-239, 2008.

[3] S. A. Razavi and M. H. Neshati, "Development of a linearly polarized cavity backed antenna using HMSIW technique," *IEEE Antennas and Wireless Propagation Lett.*, vol. 11, pp. 1307-1310, 2012.

[4] P.-S. Kildal, E. Alfonso, A. Valero-Nogueira and E. Rajo-Iglesias, "Local metamaterial-based waveguides in gaps between parallel metal plates," *IEEE Antennas and Wireless Propagation Lett.*, vol. 8, pp. 84-87, 2009.

[5] P.-S. Kildal, "Three metamaterial-based gap waveguides between parallel metal plates for mm/submm waves," *3rd European Conference on Antennas and Propagation EUCAP*, 2009.

[6] E. Rajo-Iglesias, A. U. Zaman, and P. S. Kildal, "Parallel plate cavity mode suppression in microstrip circuit packages using a lid of nails," *IEEE Mic. Wireless Comp. Lett*. vol. 20, no. 1, pp. 31–33, 2010.

[7] A. Moghimizadeh, S. Ali. Razavi and M. H. Ostovarzadeh, "Cavity backed slot antenna based on groove gap waveguide technology," *International Conference on New Perspective in Electrical & Computer Engineering*, 2016.

[8] P.-S. Kildal, A. U. Zaman, E. Rajo-Iglesias, E. Alfonso, and A. Valero Nogueira, "Design and experimental verification of ridge gap waveguide in bed of nails for parallel-plate mode suppression," *IET Microwaves Antennas Propag.* vol. 5, no. 3, pp. 262-270, Feb. 2011.

[9] A. Valero-Nogueira, M. Baquero, J. I. Herranz, J. Domenech, E. Alfonso, and A. Vila, "Gap waveguides using a suspended strip on a bed of nails," *IEEE Antennas Wirel. Propag. Lett.*, vol. 10, pp 1006-1009, 2011.

[10] E. Rajo-Iglesias and P.-S. Kildal, "Numerical studies of bandwidth of parallel-plate cut-off realized by a bed of nails, corrugations and mushroom-type electromagnetic bandgap for use in gap waveguides," *IET Microwaves Antennas Propag.* vol. 5, no. 3, pp. 282-289, Feb. 2011.

[11] N. Hassani, M. H. Ostovarzadeh, and S. A. Razavi, "Realization of a Dual Mode Filter in Ridge Gap Waveguide (RGW) Technology," *Microwave Optical Tech. Lett.*, vol. 60, pp. 1975-1979, June 2018.

[12] C. A. Balanis, *Antenna theory analysis and design*, John Wiley & Sons, 2005.